

# ACCURACY FACTORS IN MICROWAVE NOISE PARAMETER MEASUREMENTS

A. Davidson, B. Leake, and E. Strid

Cascade Microtech, Inc., P.O. Box 1589  
Beaverton, OR (503) 626-8245

## ABSTRACT

Factors contributing to microwave noise parameter measurement accuracy are examined theoretically and experimentally. It is shown that the test source impedances needn't be grouped around the impedance for minimum noise. Calibration and DUT S-parameter accuracy is shown to be important to the noise parameter accuracy. A new algorithm has been implemented which corrects for different noise source "on" and "off" impedances.

## INTRODUCTION

While noise parameter measurements are critical for low-noise microwave circuit design and device characterization, accurate means of gathering noise parameters have not been generally available. The result is that measured noise parameters are often doubted [1], FET noise modeling theories remain unverified [2], and progress in low-noise device development is generally hampered. In this paper we examine various factors contributing to inaccuracies in noise parameter measurement setups, and illustrate effective corrections.

## NOISE PARAMETER MEASUREMENT SCHEME WITH VECTOR CORRECTIONS

The classic noise-parameter measurement system uses a manual or automated tuner on each end of the device under test (DUT). The tuners are used to simulate the input and output matching networks of a low-noise amplifier stage, so the noise figure and gain can be measured directly. The optimum source and load impedances can be found by locking the tuner at its optimum setting and measuring the tuner impedance with a network analyzer. If the input tuner is set for minimum indicated noise figure, the resulting tuning condition minimizes the combined loss of the tuner and the noise contributions of DUT and second stage. Since most tuners exhibit more loss with increasing reflection coefficient, the typical result is that the indicated optimum reflection coefficient magnitude is too low [3]. Also, the second stage noise contribution is usually significant. The noise figure of the receiver is a function of the impedance the DUT presents to it (not necessarily  $Z_0$ ), and the DUT's power gain is being measured instead of its available gain if the tuner has losses.

The system block diagram in Fig. 1 (Cascade Microtech NPT18) has been used in the present work. To correct for the tuner losses, and to more accurately determine the optimal tuning conditions, the input tuner is tuned to a set of predetermined impedance points instead of searching for minima [4-6]. To improve the measurement throughput and avoid device oscillations, the output of the DUT is not tuned, but purposely terminated in the broadband low-noise amplifier. The mismatch occurring between the DUT output and the amplifier input is calculated from the DUT S-parameters and the input reflection coefficient of the receiver. To measure the DUT S-parameters and to calibrate the tuner impedances and the mismatches of the system, a vector network analyzer is switched into the DUT ports. Vector reflection information allows more accuracy than scalar approaches.

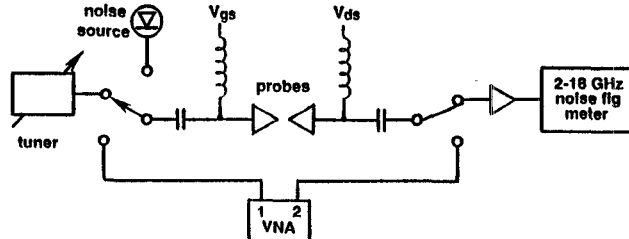


Figure 1 Combined S-parameter and noise parameter measurement system.

To calibrate the system, the vector analyzer is first calibrated at the DUT connection planes. Then, for all test frequencies, the source impedances presented to the DUT are measured for each tuner setting and for the hot and cold noise source ( $Z_{si}$ ,  $Z_{on}$ , and  $Z_{off}$ ). The available gain of the two port which connects the external calibrated hot noise source to the DUT is measured to allow transfer of the ENR calibration to the DUT. The input impedance ( $Z_2$ ) of the second stage receiver is also measured and noise parameters of the second stage calculated from noise power measurements with a through-connect between probe tips. To characterize a DUT between probe tips, its S-parameters are measured ( $DUT S_{ij}$ ), then one measurement of noise power with the hot noise source connected is made, followed by a number of similar measurements with other source impedances at ambient temperature. These measurements provide all the information necessary to calculate the overall system noise parameters ( $F_{min12}$ ,  $Y_{opt12}$ ,  $N_{12}$ ) and the DUT noise parameters and associated gain ( $F_{min1}$ ,  $Y_{opt1}$ ,  $N_1$ ,  $Gav_1$ ).

Accuracy of calculated noise parameters is improved by appropriate use of vector network analyzer calibration measurements of the noise system. Table 1 shows which type of measured quantities contribute to the intermediate results and the desired DUT noise parameters.

"Raw" measurements:	$S_{11}$	$S_{12}$	$S_{21}$	$S_{22}$	ENR	$P_{on}$	$P_{off}$
Derived parameters:							
$Z_2$					x		
$Z_{si}, Z_{on}, Z_{off}$						x	
$F_{min2}, Y_{opt2}, N_2$	x				x	x	x
$DUT S_{ij}$	x	x	x	x			
$Gav_1$	x	x	x	x			
$F_{min12}, Y_{opt12}, N_{12}$	x	x	x	x	x	x	x
$F_{min1}, Y_{opt1}, N_1$	x	x	x	x	x	x	x

TABLE 1. Relations of the basic measurements to the intermediate and final noise parameter measurements.

A direct analysis of errors in just a three-term reflection coefficient error correction [7] is complex and strongly dependent upon the DUT parameters. The noise parameter measurement system's corrections interact strongly with each other and with the DUT to create calculated results, so some means of splitting up the problem are needed. Some of the accuracy-degrading effects were simulated, and some were investigated by experimentally varying the calibration or measurement parameters.

## SOURCE IMPEDANCES: WHERE AND HOW MANY

One classic argument in noise parameter measurement is how many test source impedances to use, and where they should be on the Smith chart. A minimum of four impedances are necessary to solve for the four noise parameters  $F_{min}$ ,  $G_{opt}$ ,  $B_{opt}$ , and  $R_n$ , but more are usually used to provide averaging and to prevent singular data points.

To lend insight to the problem of how source impedances should be distributed on the Smith chart, a computer was used to simulate noise figure measurements for a wide variety of source impedance configurations. Topics of interest are how the source impedances should be distributed and how many are needed to optimize for accuracy and measurement speed.

The noise parameters of a typical FET were used to calculate noise figure at each of the given impedance points, and each noise factor was then assigned a random error ranging from  $-1\%$  to  $+1\%$ . The resulting noise figures were then used to calculate the noise parameters using a least squares routine [5]. The differences between the calculated parameters and the original parameters are then stored. For each set of conditions, the procedure was repeated 400 times and the resulting errors were RMS averaged.

The simulations presented here used configurations forming a cross shape on the Smith chart. Figure 2 shows two configurations with nine source impedances each. Parameters which describe each configuration are the maximum reflection coefficient of the outer source points ( $\Gamma_{max}$ ), the angular orientation of the configuration ( $\theta_{con}$ ), and the number of source points. In all cases, one of the points was positioned at the center of the Smith chart, while the remaining points were distributed evenly along the lines forming the cross. The position of the optimum reflection coefficient ( $\Gamma_{opt}$ ) was 0 degrees, 0.75 magnitude. The other noise parameters used ( $F_{min}$  and  $\beta$ ) are defined in Table 2.

$\theta_{con}$  was allowed to vary in the simulation because physical tuners will likely be distanced from the DUT by lengths of transmission line, causing the orientation of the configuration relative to  $\Gamma_{opt}$  to change with frequency.

Figures 3a and 3b show the errors in predicted noise parameters for  $\theta_{con} = 0$  degrees and 45 degrees, respectively, as a function of  $\Gamma_{max}$ . The  $\Gamma_{opt}$  error is the RMS of the magnitude of the vector difference between actual and predicted optima, while the other errors are RMS values of actual minus predicted parameters normalized to the actual values. An important observation is the similarity of the results for each of the two  $\theta_{con}$ . Looking at the point where  $\Gamma_{max} = \Gamma_{opt} = 0.75$ , the case for  $\theta_{con} = 0$  has  $\Gamma_{opt}$  coincident with a source impedance, while in the case for  $\theta_{con} = 45$  degrees,  $\Gamma_{opt}$  is distanced by a 0.5 vector from the closest source impedance yet actually gives slightly better accuracy.

$$F_{min} = 1.5 \text{ dB}$$

$$\Gamma_{opt} = .75 \angle 0^\circ$$

$$\beta = \frac{4R_n}{Z_0} \frac{1}{|1 + \Gamma_{opt}|^2} = 2.7$$

$$F = F_{min} + \frac{4 R_n}{Z_0} \cdot \frac{|\Gamma_{opt} - \Gamma_s|^2}{|1 + \Gamma_{opt}|^2 (1 - |\Gamma_s|^2)}$$

Table 2 Noise parameters used in simulation.

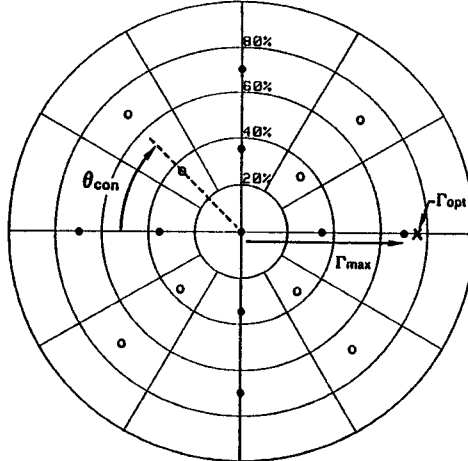


Figure 2 Two configurations used in the simulation.

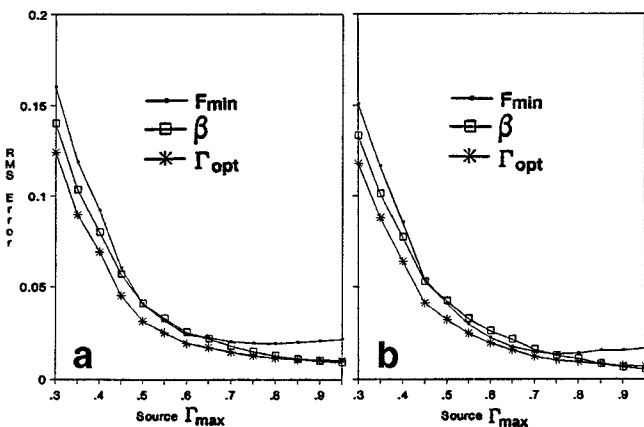


Figure 3 Errors in predicted noise parameters vs. maximum source reflection coefficient: a)  $\theta_{con} = 0^\circ$ , b)  $\theta_{con} = 45^\circ$

Also important is the improved accuracy with increasing  $\Gamma_{max}$  seen in both cases. At least when considering errors in noise figures only, measurements at large source reflection coefficients appear advantageous. Note however that reasonable accuracy may be obtained for source reflection coefficients even smaller than  $\Gamma_{opt}$ —the errors at  $\Gamma_{max} = 0.6$  are similar to the errors at  $\Gamma_{max} = \Gamma_{opt} = 0.75$ .

Another simulation was run in which an initial configuration was chosen with  $\Gamma_{max} = 0.8$ , and successive configurations were then chosen which had source points in greater proximity to  $\Gamma_{opt}$ . A scale factor was used such that for a scale factor of 0.7, for example, each point in the initial configuration moved to a point 70% of the distance between the initial point and  $\Gamma_{opt}$  (see Fig. 4). Figure 5 shows the results, where it is seen that as the configuration moves closer to  $\Gamma_{opt}$  the error in  $\beta$  increases significantly, while  $F_{min}$  and  $\Gamma_{opt}$  show slight change. This is expected since  $\beta$  describes how rapidly the noise surface varies away from  $\Gamma_{opt}$ .

Figure 6 shows the errors in predicted noise parameters as a function of the number of points in the configuration, where each configuration used had a  $\Gamma_{max}$  of 0.7 and an  $\theta_{con}$  of 45 degrees. The flatness of this curve relative to the others indicates that number of points is not of primary importance in determining the quality of a configuration.

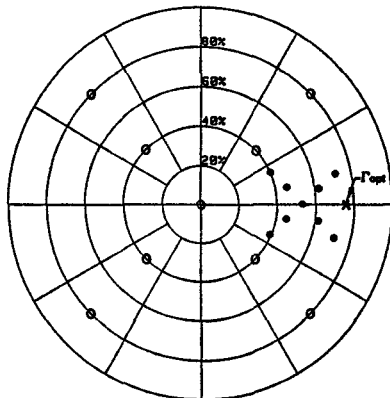


Figure 4 Two configurations: The smaller corresponds to a scale factor of 0.7, the larger a scale factor of 0.

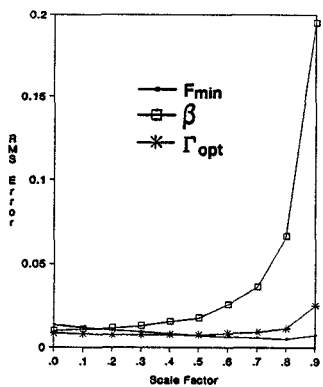


Figure 5 Noise parameter errors vs. proximity of source points to  $\Gamma_{\text{opt}}$ .

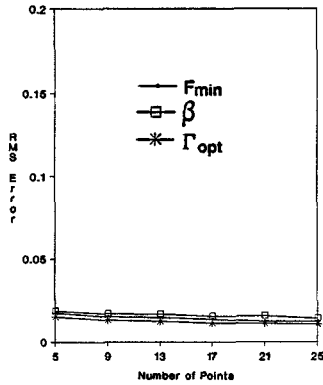


Figure 6. Noise parameter errors vs. number of source points.

The above simulations assumed measurement errors in noise figure only, which is consistent with the least squares fit which also assumes noise figure errors. If instead one assumes errors in source reflection coefficients but uses the same fitting routine, the results will change. An example of this is seen in Fig. 7, which is equivalent to Fig. 3b except that random source reflection coefficient errors ( $-.01$  to  $.01$  added to the real and imaginary parts of the reflection coefficient) were used instead of noise figure errors. The increase in errors with increase of  $\Gamma_{\text{max}}$  is expected since generally, as a source impedance gets closer to the edge of the Smith chart, the gradient of the noise surface gets steeper and errors in source reflection coefficient will result in large "effective" errors in noise figure. One

possible way to overcome this effect would be to use an orthogonal fitting routine [6] which would ameliorate source reflection coefficient errors.

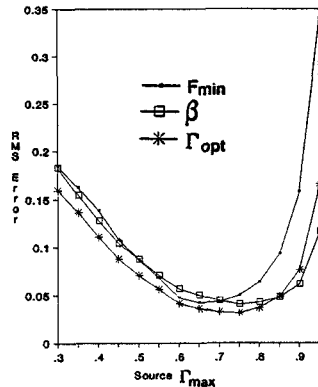


Figure 7 Noise parameter errors assuming errors in source reflection coefficients.

We can conclude from these examples that the principal concern in choosing a configuration is not the number of source impedances but rather their distribution on the Smith chart. If the points are well distributed, then the entire noise figure surface will be described accurately, and consequently the noise parameters will be accurately predicted even though measurements were not necessarily made at the optimum. Given that measurement time is proportional to number of points, there is clear advantage to fewer, well placed source impedances, which will yield good results independent of the location of  $\Gamma_{\text{opt}}$ .

Applying this notion to measured data, Fig. 8 shows  $F_{\text{min}}$  of a HEMT measured from 2 to 18 GHz using noise figures of nine source impedance points as shown in Fig. 9 for 6 GHz. Groups of eight or seven points from the same measurements were fitted and found to give  $F_{\text{min}}$  typically within 0.05 dB.

Smoothness of the measured noise parameters of a small device with frequency is often one indication of accuracy. Figure 8 shows measured  $F_{\text{min}}$  for a HEMT measured with wafer probes, where the difference from a smooth line is everywhere less than 0.1 dB.

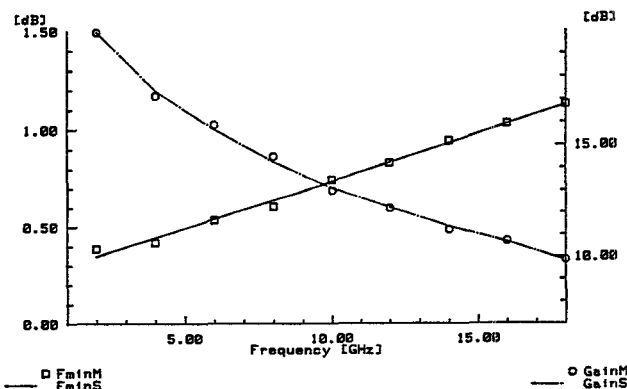


Figure 8  $F_{\text{min}}$  and associated gain of a HEMT from measured data.

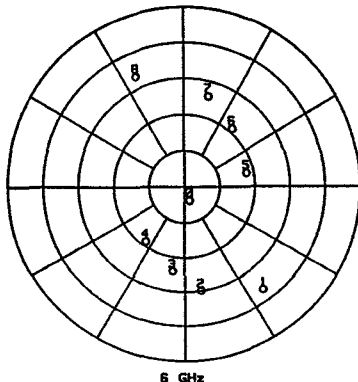


Figure 9 Configuration of source points used in measurements at 6 GHz.

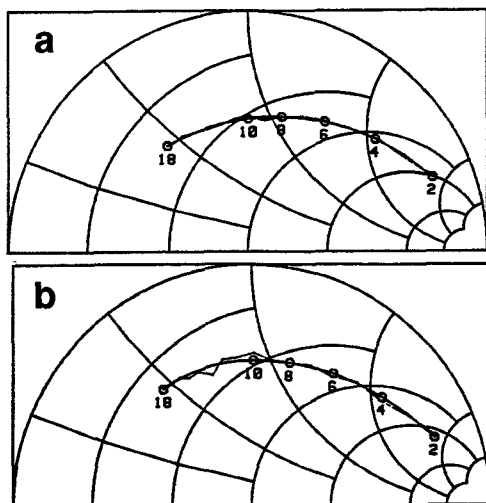


Figure 10  $F_{opt}$  of a MESFET using a) standard S-parameter calibration and b) a calibration where  $C_{open}$  was increased 10 fF.

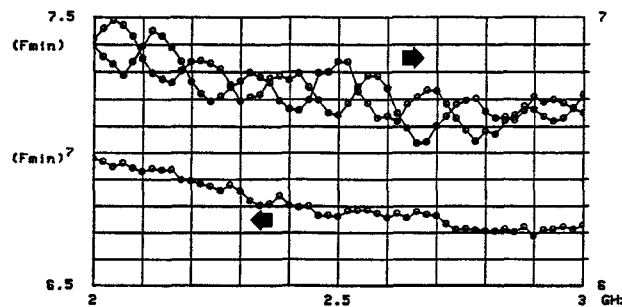


Figure 11  $F_{min}$  of an amplifier without correcting for "on"-off" noise source difference (top curves, right-hand scale) and with a correction (bottom curve, left-hand scale).

## S-PARAMETERS

### S-Parameter Accuracy

The accuracy of the S-parameters used to calibrate the input tuner and to measure the DUT S-parameters are of prime importance to

the noise parameter accuracy. Figure 10 demonstrates one effect of the S-parameters on the noise parameters. In Fig. 10a, the device was measured with a normal S-parameter calibration. Figure 10b shows the same device and bias condition, but with a different S-parameter calibration. The different calibration changed only the open circuit capacitance definition by 10 fF. The optimal reflection coefficients shifted up, as is experienced with S-parameter measurements[7]. In addition there is an extra scatter of the points which cannot be due to the DUT.

Also, effects such as probe placement on the DUT are readily observable. Different probe placement causes a change in inductance in the transition to the DUT, causing a shift in optimal source angles equal to the shift that probe placement causes in S-parameter measurements [8].

### Noise Source Impedance Variation

It is well known that the "on" and "off" impedances of typical solid-state noise sources are not identical, and that this causes noise figure measurement errors [9-10]. Figure 11 shows the result of measuring an amplifier's minimum noise figure with a 15 dB ENR noise source directly on the tuner. In this test the vector difference between the "on" and "off" reflection coefficients is about 0.05. The top two curves were made with different electrical lengths between the noise source and the DUT. The ripples of  $F_{min}$  with frequency correspond to rotation of the vector difference between the "on" and "off" reflection coefficients. The lower curve resulted from similar measurements, but shows how the ripples disappeared using a new algorithm which exactly corrects for the shift in noise source impedance.

### CONCLUSIONS

We have investigated various factors responsible for inaccuracies in microwave noise parameter measurements, including the number of source admittances, the position of the admittances on the Smith chart in relation to DUT parameters, the accuracy of the source admittances and device S-parameters, and the effect of changing noise source impedances. It is too early to conclude that this is an exhaustive list of relevant factors, and too early to conclude exactly how they interact with each other. However, we have shown the feasibility of noise parameter measurements with less than 0.1 dB variations of  $F_{min}$  with frequency with high throughput.

### REFERENCES

- [1] M. Pospieszalski, et.al., "Comments on 'Design of Microwave GaAs MESFETs for Broadband, Low-Noise Amplifier'", *IEEE Trans on MTT*, Vol. MTT-34, No.1, Jan. 1986, p. 194.
- [2] A. Cappy, "Noise Modeling and Measurement Techniques", *IEEE Trans. on MTT*, Vol. MTT-36, No. 1, Jan. 1988, pp. 1-10.
- [3] E. Strid, "Measurement of Losses in Noise-Matching Networks", *IEEE Trans. on Microwave Theory and Techniques*, Vol. MTT-29, No. 3, pp. 247-252, March 1981.
- [4] R.Q. Lane, "The Determination of Device Noise Parameters", *Proc. IEEE (letters)*, Vol. 57, Aug 1969, pp. 1461-1462.
- [5] G. Caruso and M. Sannino, "Computer-Aided Determination of Microwave Two-Port Noise Parameters", *IEEE Trans. on MTT*, Vol. MTT-26, Sept. 1978, pp. 639-642.
- [6] M. Mitama and H. Katoh, "An Improved Computational Method for Noise Parameter Measurement", *IEEE Trans. on MTT*, Vol. MTT-27, June 1979, pp. 612-615.
- [7] Cascade Microtech Model 42 Operation Manual, Chap.4. Cascade Microtech, Beaverton, Or.
- [8] K. Jones and E. Strid, "Where are my on-Wafer Reference Planes?", *IEEE ARFTG Digest of Papers*, Dec. 1987.
- [9] E. Strid, "Noise Measurements for Low-Noise GaAsFET Amplifiers", *Microwave Systems News*, Part I, pp. 62-70, Nov. 1981, Part II, Dec. 1981.
- [10] N.J. Kuhn, "Curing a Subtle but Significant Cause of Noise Figure Error", *Microwave J.*, Vol. 27, June 1984, pp. 85-98.